International Journal of Engineering & Technology, 7 (2.33) (2018) 139-144

International Journal of Engineering & Technology

Website: www.sciencepubco.com/index.php/IJET

Research paper

Design fabrication and performance analysis of length morphing rotor blade

G. Saravanan [1], Vinoth Kumar Annamalai [1] *, N. Bharath [1], Antonio Kevin [2], G. Rahul Teja [2], Neil Steven Anto [2]

[1] Assistant Professor, Department of Aerospace Engineering, SRMIST, Chennai, 603203 Tamil Nadu, India
[2] Student, Department of Aerospace Engineering, SRMIST, Chennai, 603203 Tamil Nadu, India
**Corresponding author E-mail: vinothkumar.ae@gmail.com*

Abstract

The present work deals with helicopter theory involving the study, design and fabrication of the helicopter rotor blades with the length-morphing mechanism. The research of the rotor blades has enabled in a proper understanding of the aerodynamics and design of the same. The thrust produced by a blade is proportional to its area, and for every motor RPM, maximum thrust efficiency is achieved for a discrete length of the rotor blade. Facing this complexity, designers compute an optimal length for the average motor RPM while designing the heli-copter blades. Acknowledging the challenges, Length-Morphing rotor blades targeting maximum thrust efficiency for each motor RPM was developed with the aid of knowledge in Blade Element Theory. The rotor blade was designed and fabricated to be driven by the centrifugal force from the motor. The rotor blade was divided into fixed inboard section and sliding outboard part in a span-wise di-rection. The analy-sis was carried out to study and comprehend the operating conditions of the length-variable rotor during revolutions and to derive the design variables of extension-spring and rotor weight. Variation of thrust concerning the length of the rotor blade was studied, and the setup was fabricated. The project aims to enable maximum rotor blade thrust efficiency for each RPM of the motor by varying the length of the rotor blade and computing the performance characteristics of the same.

Keywords: Blade Element Theory; Centrifugal Force; Extension-Spring; Length Morphing Mechanism; Thrust; Efficiency.

1. Introduction

The performance of the helicopter entirely depends on the length of the rotor blade. In order to produce higher thrust, the helicopter rotor blade angle is varied, but after an angle the rotor blade stalls. So, to create the higher thrust after the maximum angle of attack, a concept was proposed in which the length of the rotor blade will be increased based on the rotational speed of the rotor.

Till now most of the research is concentrated on the morphing of the airfoil to produce more thrust. For morphing the shape of the airfoil, it requires a lot of control input, and a sophisticated control mechanism is necessary to provide the desired shape and size of the airfoil, which in turn increases the number of control input of the control system of the aeroplane. Thus, the concept of length morphing rotor blade based on the rotational speed works on the principle of the centrifugal force acting on the spring, which in turn increases the length of the rotor blade.

In Sikorsky, a variable diameter rotor was used, in which the rotor similar to the conventional helicopter, but blades are of the telescope in nature during the flight to increase or decrease rotor disk area by increasing or decreasing the length of the rotor. In Sikorsky, a complex system of differential gears, extension rods and retraction brakes, and screw jacks are used to extend and retract the rotor blades, which in turn increases the complexity of the system.

So, in our proposed work, the length of the rotor was varied by attaching the spring at the end of each rotor blades. Thus, based on the rotational speed and inertial weight of the rotor blades a cen-trifugal force is generated at the outer part of the telescopic rotor blade. The centrifugal force acts on the spring and tends to extend outwards, which in turn extends the telescopic rotor. Finally, the diameter of the rotor disk increases , which also increases the thrust produced by the rotor blades to improve the performance of the helicopter rotor blades.

2. Telescopic mechanism of the rotor blade

The rotor blade design has several challenges, of which the big-gest problem is not being able to produce the maximum thrust efficiency for every motor RPM. The designers face this complex-ity while choosing the length of the rotor blades for the helicopter. For every motor RPM, there exists a distinct length which will give the maximum thrust efficiency which can be theoretically computed from the Blade Element Theory and Momentum Theory. So, say the motor is operating within a predefined RPM range; designers choose an optimum speed and fix the length of the blade according to that RPM. It merely means that the rotor blades of the helicopter failed to give maximum thrust efficiency for every motor speed. This calls for the need of a telescopic model in a rotor blade where the blade can automatically morph its length according to the motor speed thereby maximising the overall thrust efficiency of the blade. This is made practicable by separat-ing the rotor blade into two sections; a fixed inboard section and a sliding outboard.

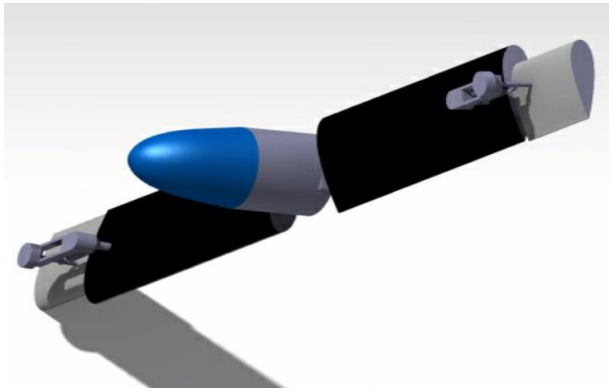

Fig. 1: Telescopic Mechanism of the Rotor Blade.

The length morphing mechanism is made realisable by using a spring-mechanism wherein the spring uses the free centrifugal force provided by the angular velocity of the motor to expand and compress according to the motor RPM. Therefore, the inboard section of the rotor blade is static, and the outboard part which is connected to the inboard using a spring changes its length according to the speed of the motor. Hence, the entire length of the rotor blade varies for every motor speed, thereby enabling the propeller blade of the helicopter to achieve maximum thrust efficiency for every RPM of the motor which is controlled by the regulator.

3. Design of aero foil and rotor blades

3.1. Selection of aerofoil

The factors to be considered for the selection of the aerofoil are thinner and less cambered airfoils so that a propeller should be designed to prevent supersonic flow by choosing the right airfoil thickness and the correct diameter. The Drag divergence Mach number also affects the airfoil section, so Reynolds number must be considered for increasing the drag divergence Mach number, so the airfoil's angle of attack can be raised higher, and the rotational speed of the rotor can also be increased by choosing the airfoil having high Drag divergence Mach number.
Considering the above facts, the fabricator's ease and availability, the aerofoil was chosen for the rotor blade was NACA 0024.
The coordinates of the aerofoil were taken from designfoil.com and were plotted on a graph.

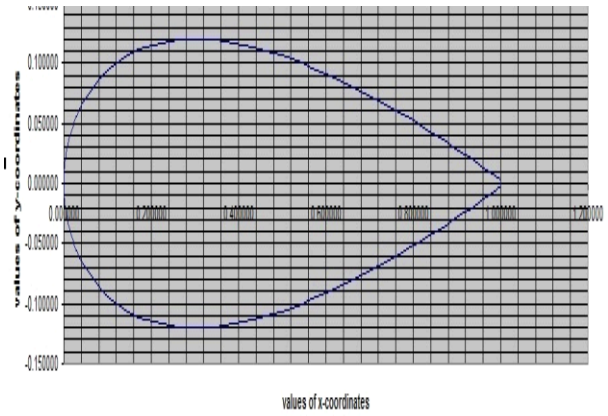

Fig. 2: NACA 0024 Airfoil Profile.

3.2. Design and selection of spring

Steel spring is an elastic object which is used to store mechanical energy applied on it. Spring index plays a significant role in the selection of Spring and is represented 'C'. Spring index is defined as the ratio of Diameter of the spring to the diameter of the spring coil, and the value should vary from 4-12 for continuous use.

$$C = \frac{D_S}{d_s}$$

Where
D_S=Diameter of the spring
d_s= diameter of the spring coil

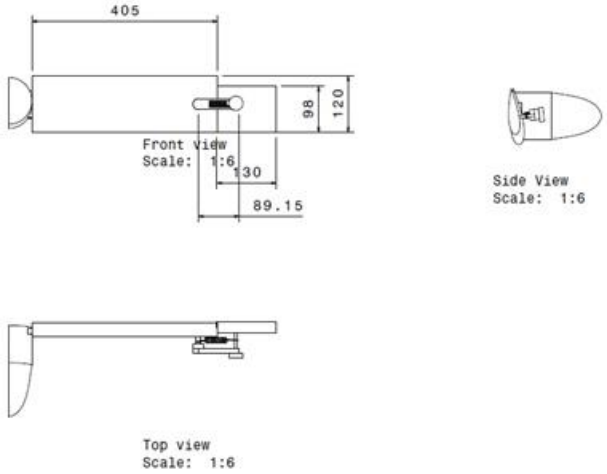

Fig. 3: 3-View Diagram of a Single Rotor Blade.

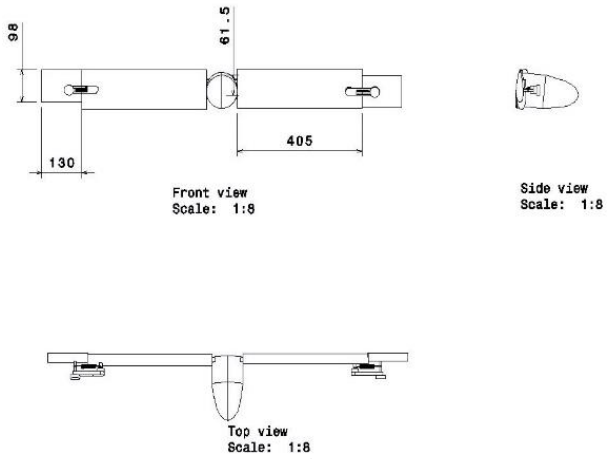

Fig. 4: 3-View Diagram of the Rotor Blade System.

3.3. Outboard rotor blade

The outboard rotor blade is the outer section of the airfoil which is connected to the hub. It is a hollow surface which permits the movement of the inner rotor blade using a guide. Thus, the movement of the inboard blade within the outboard blade is constrained by the guide in its preferred axis.

Table 1: Specifications of Outboard Rotor Blade

Specifications:	
Material	Mild steel
Outer airfoil length	40.5cm
Outer surface length	28cm
Weight	1.016kg
Outer airfoil rod length	18cm
Rod (guide) height	2.5cm
Maximum outer airfoil thickness	4cm

3.4. Inboard rotor blade

The inboard rotor blade is the one which is the spring action when it is unlocked and allowed to expand by the centrifugal force. The inboard rotor blade is also facilitated with a guide shaft so that it moves within the confined space when under spring action.

Table 2: Specifications of Inboard Rotor Blade

Specifications:	
Material	Mild Steel
Inner airfoil length	30cm
Joint rod length	17cm
Joint rod height	2cm
Airfoil surface length	22cm
Airfoil weight	0.622Kg

3.5. Provision for telescopic movement

Since the inboard section must slide inside the outboard airfoil, a rectangular hollow shaft was welded inside the outer airfoil. The inner airfoil was fabricated with another hollow shaft accordingly, which enables the telescopic movement of the internal airfoil inside the outer one due to spring action.

3.5.1. Fixing of rotor blades to the hub

A stand of 30 inches height was chosen. A hub was welded to the support stand where the propeller blades are to be mounted. The two telescopic blades were riveted to the centre using bolts and nuts.

Fig. 5: Provision for Telescopic Movement.

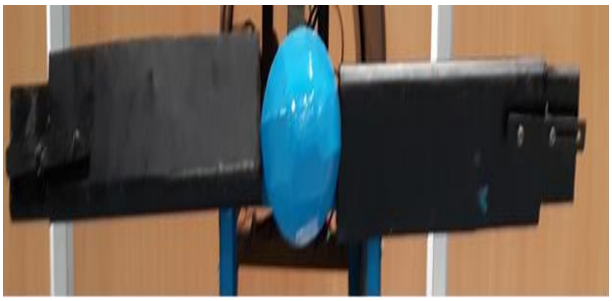

Fig. 6: Rotor Blades to the Hub

4. Experiment

4.1. Length morphing rotor blade test rig

The entire setup diagram consists of the rotor blade with length morphing mechanism actuated using a spring. They are connected to the hub. A shaft of length 42cm and 1.11 cm diameter connects the motor to the hub. Thus when the engine is turned on, the blades rotate about the hub and therefore tend to produce forward thrust. This causes a net forward force on the engine to move along with the hub. The engine is provided with a roller bed to facilitate smooth movement. The forward motion is restricted by the load cell which is kept along the sliding path. Thus, the load cell measures the forward thrust produced by the rotor blade. The AC motor is provided with and an electric circuit board which regulates the voltage by which the RPM can be controlled. The tachometer is used to measure the RPM and provisions are made to make the motor run at 50,100,150 and 200 RPMs.

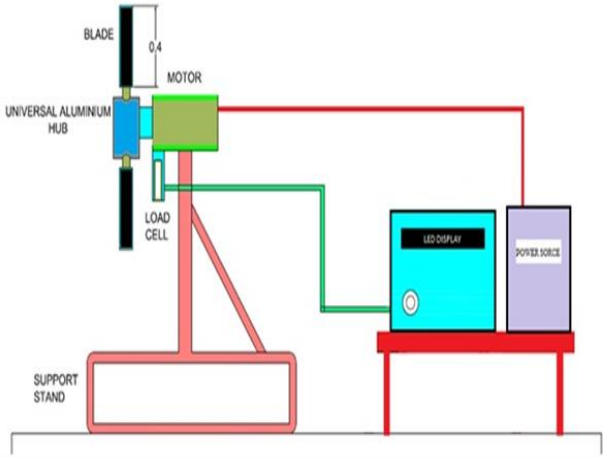

Fig. 7: Setup Diagram when the Spring is Locked.

Initially, the spring is fastened and the engine is operated. The motor can run at different RPMs using the voltage regulator, and the corresponding readings of thrust are obtained from the load cell and are tabulated.
Then, the spring is unlocked, and the same process is repeated. The readings are tabulated and compared.

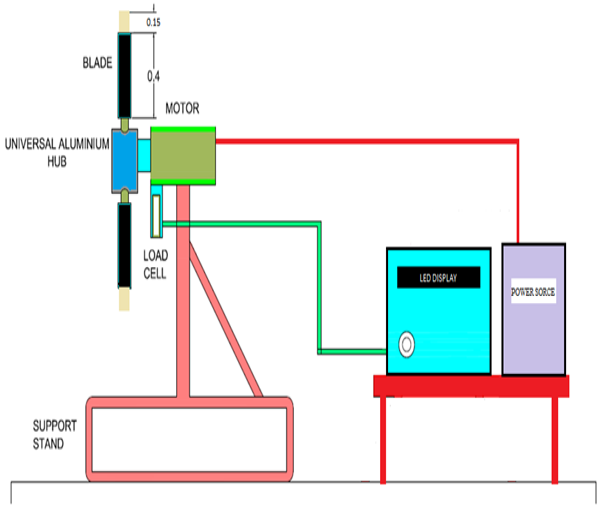

Fig. 8: Setup Diagram when the Spring is Unlocked

IGBTs, which converts a fixed voltage, fixed frequency alternating current (AC) electrical input supply to obtain a variable voltage in output delivered to a resistive load. This different voltage output is used for dimming street lights, varying heating temperatures in homes or industry, speed control of fans and winding machines and many other applications, in a similar fashion to an autotransformer. Voltage controller modules come under the purview of power electronics.
The calculations are done for two cases. In the first case, the spring is locked. Thus, the inboard rotor blade is fixed to the outboard blade and is not allowed to expand. From the known values of distance travelled by the blade, radius of the blade and the period, the values of blade tip velocity and mass flow rate are found out. Then the motor can run at different RPMs, and the values of angular velocity, centrifugal force and thrust are computed for each angular velocity. The values are tabulated. In the second case, the spring is unlocked, and the same process is repeated to find the values of blade tip velocity, mass flow rate, centrifugal force and thrust.
Case 1: When spring is locked
Time period:

$$T = 60/N$$

Where
T= time period
N=number of rotations per minute
D= distance travelled by the blade (m)
r= radius of the rotor blade (m)
v= Blade tip velocity (m/s)
Centrifugal force:

$$\omega = \frac{2\pi N}{60}$$

Where

N=number of rotations per minute

$$C_f = mr\omega^2 = \frac{mv^2}{r}$$

Where

m= mass of the inner airfoil (kg)
r= radius of the rotor blade (m)
Thrust:

$$F = \frac{(\rho\pi d^2)}{4} \times \left[\left(\frac{NP^2}{60}\right) - \left(\frac{NP^2}{60}\right)V_s\right] \times \left(\frac{D\eta}{P}\right)^{1.5}$$

Here, F= dynamic thrust and is forward airspeed since our setup is static we need to neglect to find static thrust so
Modified formula to find static thrust as given below

$$F = \frac{(\rho\pi d^2)}{4} \times \left[\left(\frac{NP^2}{60}\right)\right] \times \left(\frac{d\eta}{P}\right)^{1.5}$$

Where
F=static thrust (N)
N= number of rotations per second
d= diameter of the rotor blade
p=pitch of the rotor blade
η =assumed as 100%=1

5. Results and discussions

The following are the list of values obtained using theoretical calculations and experimental validation. In all these cases, the voltage regulator is used to regulate the motor angular speed at 50, 100, 150 and 200 RPM. The values of blade tip velocity, mass flow rate, centrifugal force and thrust are calculated for each RPM and are tabulated. The graphs are plotted, the variation is observed, and the inference is given.

5.1. Case 1: when the spring is unlocked

Table 3: Variation of Blade Tip Velocity with Motor RPM

RPM	Time period (s/rev)	Radius of the rotor blade (m)	Distance travelled by the rotor blade (m)	Blade tip velocity (m/s)
50	1.2	0.5625	3.53429	2.945
100	0.602	0.57	3.58141	5.9485
150	0.4	0.575	3.6128	9.032
200	0.3	0.5775	3.5971	11.99033

Table 3 shows the values of blade tip velocity at different RPMs of the motor. At different angular speed, the spring expands, and the length is measured by using a high-speed camera. The distance travelled by the blade is calculated using the radius of one blade. Knowing, the time period, the blade tip velocity is calculated. It is seen that the blade tip velocity increases as we increase the motor RPM

Table 4: Variation of Mass Flow Rate with Motor RPM

RPM	Area (m^2)	Blade tip velocity (m/s)	the mass flow rate (kg/s)
50	0.994	2.945	3.5859
100	1.02	5.9485	7.4326
150	1.0386	9.032	11.4912
200	1.049	11.99033	15.407

Table four shows that the Mass flow rate of air passing through the blade at lower RPM is higher than the mass flow rate of air passing through the expanded blades at higher RPM. This is due to the higher blade tip velocity at higher angular speeds compared to lower ones, which allows more air to pass through the blade thereby giving a higher thrust.

Table 5: Variation of Centrifugal Force with Motor RPM

RPM	Mass of the rotor blade (kg)	Radius of the rotor blade (m)	Angular Velocity of the rotor blade (rad/s)	Centrifugal force (N)
50	0.0652	0.5625	5.235	1.005
100	0.0652	0.57	10.47	4.073
150	0.0652	0.575	15.7	9.24091
200	0.0652	0.5775	20.94	16.51072

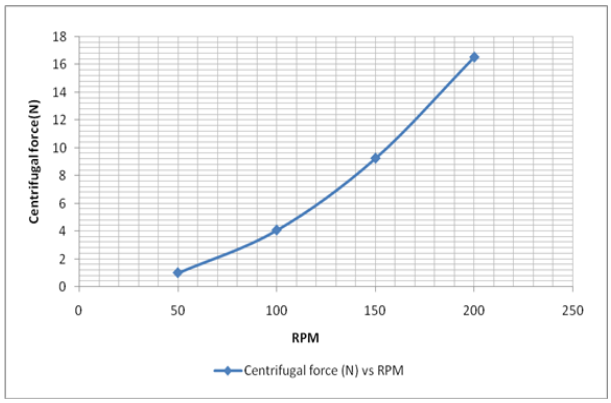

Fig. 9: Variation of Centrifugal Force with Motor RPM.

Inference: From figure 9, the centrifugal force is found to be increasing with the RPM of the motor. This means that more force acts on the spring when the motor is run at higher speeds. Therefore, the spring tends to expand, thereby increasing the length of the rotor blade as well. Since the AC motor starts slow, the initial centrifugal force is found to be lesser than at higher speeds.

Table 6: Variation of Thrust Produced by the Length Morphing Rotor Blade with Motor RPM

RPM	Thrust(N)	Thrust(kg)
50	1.79	0.183
100	4.606	0.47
150	9.114	0.93
200	16.17	1.65

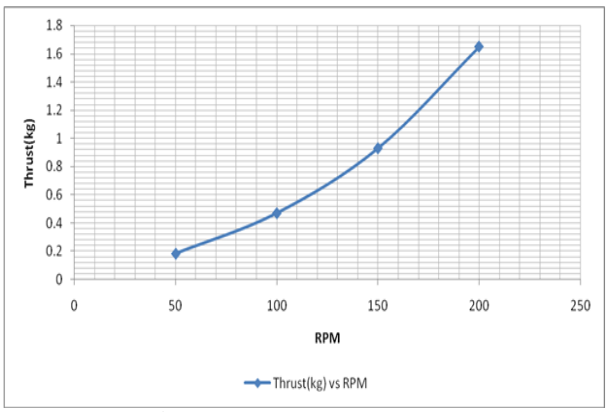

Fig. 10: Variation of Thrust Produced by the length-Morphing Blade with RPM.

Inference: From figure 10, it is found that the thrust of the rotor blade is increasing when the blades are running at higher RPM. This is because, at higher speeds, the blades rotate faster, thereby increasing the mass flow rate of air flowing against it. This causes an increase in the forward load applied to the blade which tends to slide the entire setup forward. The motion of the blade is restricted by the load cell which is kept between the motor and the blade. Thus, the load cell calculating the load applied to it shows that higher load is acting on it when the RPM of the motor is higher. The shape of the graph curves because Thrust is a function of the square of motor speed.

5.2. Case 2: when the spring is locked

The radius of the blade at locked at 0.55m and the distance travelled by the blade (2πr) is found to be 3.55m.

Table 7: Variation of Blade Tip Velocity with the Motor RPM

RPM	Time period(sec/rev)	Blade tip velocity(m/s)
50	1.2	2.879
100	0.602	5.74
150	0.4	8.6375
200	0.3	11.519

Table [7] shows that the blade tip velocity increases with the motor RPM. However, it is observed from Table 7.1 that the blade tip velocity has reduced when the spring is locked. In both these conditions, the blade tip velocity varies linearly but the distance travelled by the blade is higher when the spring is unlocked.
The area travelled by the blade (πr2) under fixed spring condition is found to be 0.95m2.

Table 8: Variation of Mass Flow Rate with RPM

RPM	Blade tip velocity(m/s)	the mass flow rate
50	2.879	3.351
100	5.74	6.681
150	8.637	10.054
200	11.519	13.4092

Table [8] shows that the mass flow rate increases with the increase in motor speed. However, it is observed from Table 4, that the mass flow rate has reduced when the spring is in a locked condition. In both these cases, the mass flow rate increases linearly but the blade tip velocity is lesser at the locked condition, therefore, enabling secondary air to pass through the blade and hence decreasing the mass flow rate. While calculating the centrifugal force, we find the mass of the rotor blade at fixed condition to be 0.0652 kg and the radius of the blade is 0.55m

Table 9: Variation of Centrifugal Force with Motor RPM for locked spring

RPM	Angular velocity of the rotor blade (rad/s)	Centrifugal Force (m)
50	5.235	0.9827
100	10.47	3.931
150	15.7	8.839
200	20.94	15.724

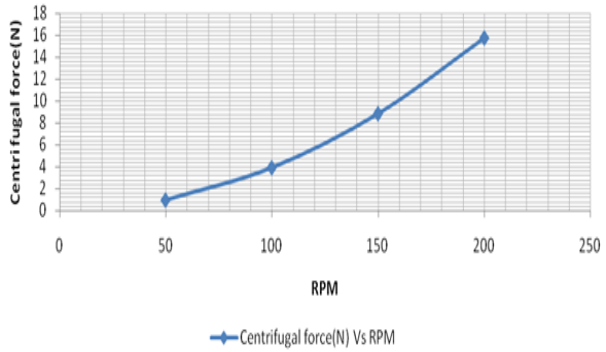

Fig. 11: Variation of Centrifugal Force with RPM for locked Spring.

Inference: It is observed from Table [5]. That the Centrifugal force has reduced when the spring is in a locked condition. In both these cases, the centrifugal increases slowly at first due to slow starting speed of the motor. But the radius in the unlocked state is higher than that of the locked state because when the motor is run, the spring expands according to the speed and the inboard rotor blade comes out of the outboard blade. Therefore, in a locked condition, the radius (in mrω2) is lesser than that of the unlocked state.

Table 10: Variation of Thrust Produced by the Rotor Blade in Locked Spring Condition with RPM of the Motor

RPM	Thrust(N)	Thrust(kg)
50	0.98	0.1
100	3.704	0.378
150	8.23	0.84
200	14.7	1.5

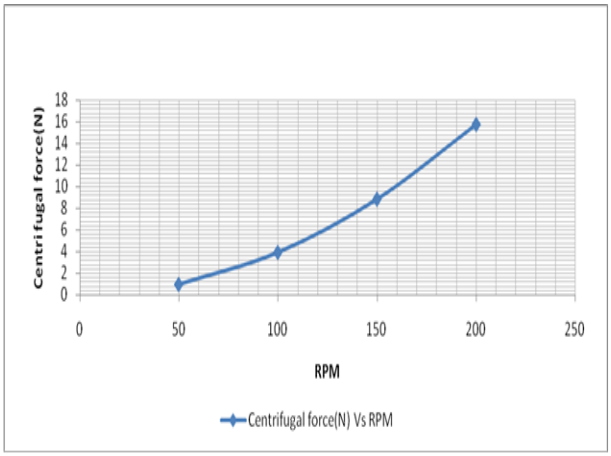

Fig. 12: Variation of Thrust Produced by the Rotor Blade in Locked Spring Condition with RPM of the Motor.

Inference: From the table 10 and figure 12, it is found that the thrust of the rotor blade is increasing when the blades are running at higher RPM. This is because, at higher speeds, the blades rotate faster, thereby increasing the mass flow rate of air flowing against it. This causes an increase in the load cell reading which is kept between the motor and the blade. Thus, a higher load is acting on it when the RPM of the motor is higher.

Table 11: Experimental Variation of Thrust with RPM of the Motor

RPM	Thrust for locked spring condition (kg)	Thrust for unlocked spring condition (kg)
50	0.05	0.183
100	0.3	0.47
150	0.7	0.93
200	1	1.65

6. Conclusion

The experiment was conducted at two different constraints. Firstly, the spring of the setup was locked, and the readings were taken. They were compared theoretically. It was followed by the limitation in which the spring could expand based on the centrifugal force of the motor. The values were compared experimentally.

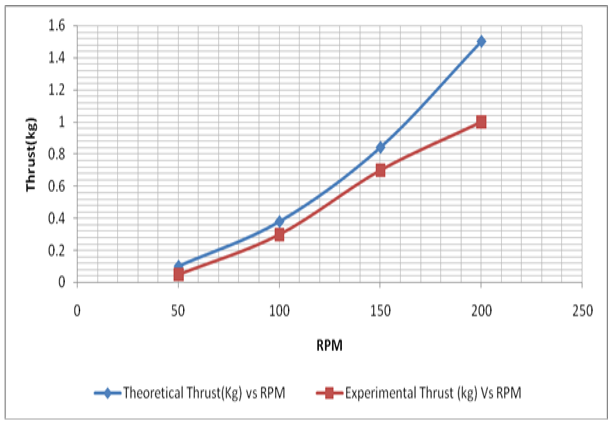

Fig. 13: Experimental and Theoretical Comparison of Thrust Variation with RPM for Locked Spring.

Inference: The above graph shows the comparison of Thrust Variation with RPM for locked spring theoretically and experimentally. The thrust is found to be varying more theoretically. This is because the thrust was calculated using 100% efficiency theoretically and the same could not be achieved practically.

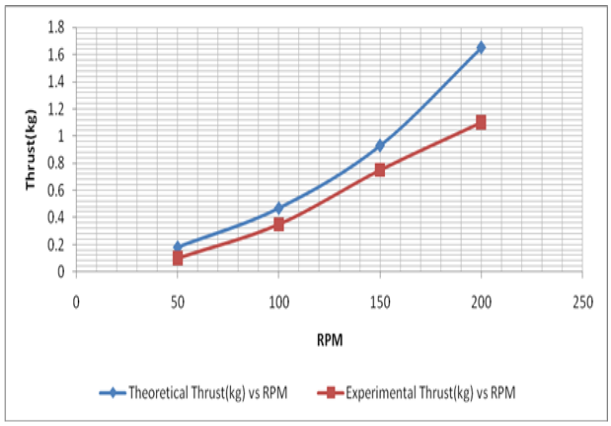

Fig. 14: Experimental and Theoretical Comparison of Thrust Variation with RPM for Unlocked Spring.

Inference: The above graph shows the comparison of Thrust Variation with RPM for unlocked spring theoretically and experimentally. The thrust is found to be varying more theoretically again. This is still because the thrust was calculated using η=one theoretically and the same could not be achieved practically.

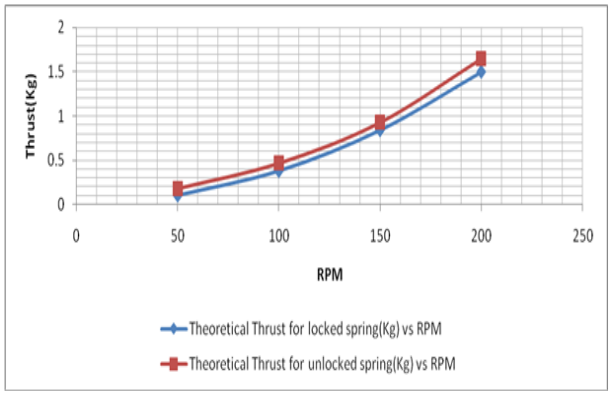

Fig. 15: Theoretical Comparison of Thrust Variation with RPM in locked spring and Unlocked Spring.

Inference: The Thrust is found to be increasing when the Length-morphing rotor blade mechanism is applied to a standard rotor blade system, theoretically. The graph forms a curve because thrust is found to be a function of the square of RPM. This chart shows that the length-morphing mechanism can achieve maximum thrust efficiency for every RPM.

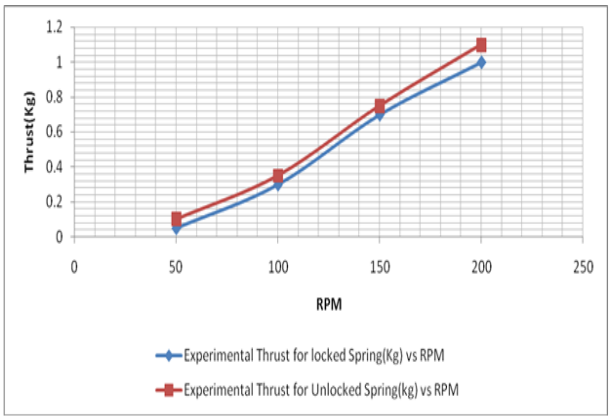

Fig. 16: Experimental Comparison of Thrust Variation with RPM in Locked Spring and Unlocked Spring.

Inference: The Thrust is found to be increasing when the Length-morphing rotor blade mechanism is applied to a standard rotor blade system, experimentally. The graph forms a curve because thrust is found to be a function of the square of RPM. This figure shows that the length-morphing mechanism can achieve maximum thrust efficiency for every RPM.

Thus, the thrust is found to be increasing when the spring is unlocked, and the length morphing mechanism is applied during both theoretical and experimental research

References

[1] Johnson Cutler, "Design and Control of an Autonomous Variable-Pitch Quad rotor Helicopter by Mark" (September 2012) pp. 270-276

[2] Dr. Adeel Khalid, Development and Testing of Variable Pitch Propeller Thrust Measurement Apparatus Freshmen Research Project, 2012

[3] John B. Brandt and Michael S. Selig "Propeller Performance Data at Low Reynolds Numbers" (January 2011)

[4] Raymer, D. P., Aircraft Design: A Conceptual Approach, 3rd ed., AIAA education series, AIAA, Virginia, 1999, pp. 15-29 and 379-400.

[5] Raphael Cohen, David Miculescu, Kevin Reilley, Mehrdad Pakmehr, Eric Feron "Performance Optimization of a DC Motor Driving a Variable Pitch Propeller"

[6] Blake. A. Moffit and Thomas. H. Bradley "Validation of vortex propeller theory for UAV design with uncertainity Analysis", 2001

[7] Richard Eppler and Martin Hepperel "A procedure for Propeller Design by Inverse Methods", 1998, pp.450- 478

[8] Grasmeyer, J. M., Keennon, M. T., "Development of the Black Widow Micro Air Vehicle," AIAA-2001-127, Aerospace Sciences Meeting and Exhibit, 39th, Reno, NV, Jan 2001